

Histamine treatment induces rearrangements of orthogonal arrays of particles (OAPs) in human AQP4-expressing gastric cells

Monica Carosino,¹ Giuseppe Procino,¹ Grazia Paola Nicchia,¹ Roberta Mannucci,² Jean-Marc Verbavatz,³ Renée Gobin,³ Maria Svelto,¹ and Giovanna Valenti¹

¹Dipartimento di Fisiologia Generale ed Ambientale, Università degli Studi, 70126 Bari, Italy

²Sezione di Medicina Interna ed Oncologia, Dipartimento di Medicina Clinica e Sperimentale, Università degli Studi, 06100 Perugia, Italy

³Service de Biologie Cellulaire, Centre d'Etudes de Saclay, F-91191 Gif sur Yvette Cedex, France

To test the involvement of the water channel aquaporin (AQP)-4 in gastric acid physiology, the human gastric cell line (HGT)-1 was stably transfected with rat AQP4. AQP4 was immunolocalized to the basolateral membrane of transfected HGT-1 cells, like in native parietal cells. Expression of AQP4 in transfected cells increased the osmotic water permeability coefficient (P_f) from $2.02 \pm 0.3 \times 10^{-4}$ to $16.37 \pm 0.5 \times 10^{-4}$ cm/s at 20°C. Freeze-fracture EM showed distinct orthogonal arrays of particles (OAPs), the morphological signature of AQP4, on the plasma membrane of AQP4-expressing cells. Quantitative morphometry showed that the density of OAPs was $2.5 \pm$

0.3% under basal condition and decreased by 50% to $1.2 \pm 0.3\%$ after 20 min of histamine stimulation, mainly due to a significant decrease of the OAPs number. Concomitantly, P_f decreased by $\sim 35\%$ in 20-min histamine-stimulated cells. Both P_f and OAPs density were not modified after 10 min of histamine exposure, time at which the maximal hormonal response is observed. Cell surface biotinylation experiments confirmed that AQP4 is internalized after 20 min of histamine exposure, which may account for the downregulation of water transport. This is the first evidence for short term rearrangement of OAPs in an established AQP4-expressing cell line.

Introduction

The general assumption in the gastrointestinal tract is that water transport occurs as a result of active ion transport, which creates the osmotic driving force for water movement. In the stomach, gastric juice is secreted mainly by fundic glands containing mucus cells, chief cells, and parietal cells, producing mucus, pepsinogen, and hydrochloric acid, respectively. Gastric juice is a solution consisting mainly of H^+ , Cl^- , K^+ , HCO_3^- , and water secreted at a rate of ~ 2 liters per day (Koyama et al., 1999; Ma and Verkman, 1999). However, the pathway for water transport driven by activation of acid secretion is still undefined. Activation of acid secretion is accompanied by extensive morphological changes in parietal cells. In resting parietal cells, the enzyme responsible for gastric acid secretion, H^+/K^+ -ATPase, is -1.

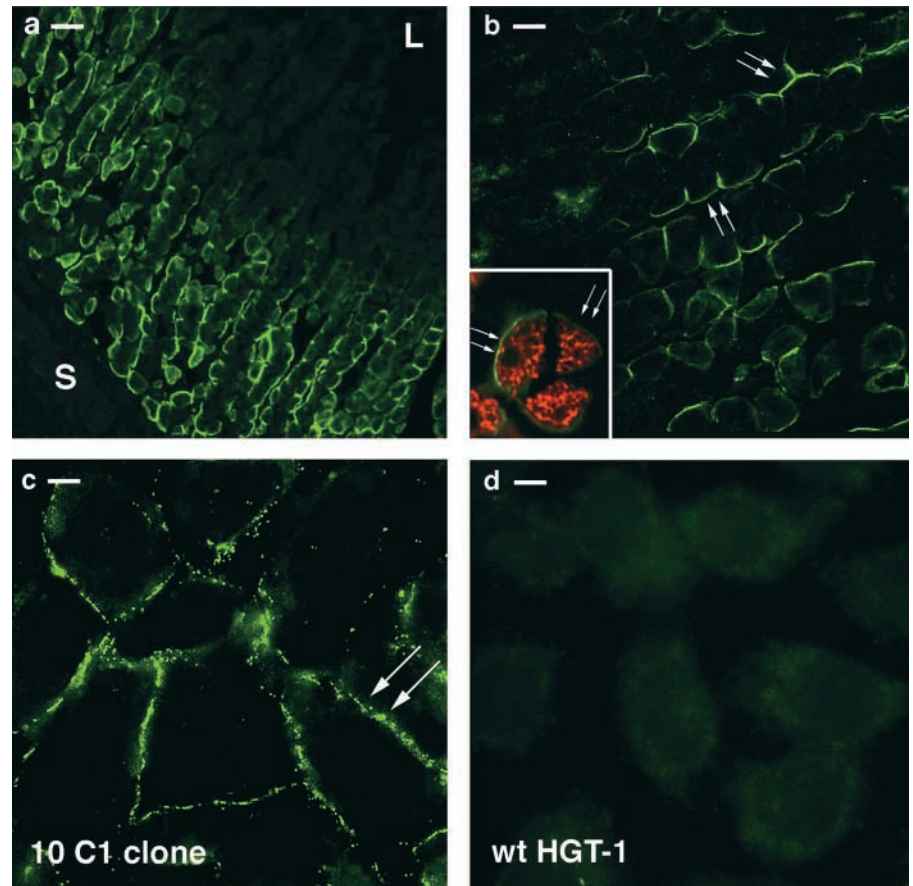
Stimulation of parietal cells causes a cytoskeletal reorganization and a fusion of tubulovesicles thus recruiting func-

tional pumps to the expanded microvillar surface. The gastric juice has a low pH and a widely varying osmolality, yet the epithelial cells lining the stomach must maintain a relatively constant intracellular osmolality and pH. These considerations suggest that the gastric apical membrane must maintain a low permeability to water so that the gastric epithelial cell is afforded some protection against abrupt changes in cell volume. The gastric apical membrane is relatively water-tight and exhibits low permeability to water (Priver et al., 1993). These properties are likely to be essential to the ability of this membrane to perform its barrier function. The stomach is a tight epithelium, which predicts a low paracellular water permeability. On the other hand, the identification of a member of the AQP family in the stomach would suggest a transcellular water movement through the gastric epithelium. The water channel AQP4 is so far the only AQP identified in the stomach. Rat AQP4 was immunolocalized to the basolateral membranes of gastric parietal cells (Frigeri et al., 1995). A human AQP4 homologue was cloned from stomach and immunolocalized to both parietal cells and chief cells (Misaka et al., 1996).

Address correspondence to Giovanna Valenti, Dipartimento de Fisiologia Generale ed Ambientale, Via Amendola 165/A, 70126 Bari, Italy. Tel.: 39-080-544-3444. Fax: 39-080-544-3388. E-mail: g.valenti@biologia.uniba.it

Key words: aquaporin; stomach; water channel; histamine; H^+/K^+ -ATPase

Figure 1. Immunofluorescence localization of AQP4 in frozen section of rat stomach. (a) AQP4 was found in the basal region of fundic glands (S, serosa; L, lumen). (b) As shown at higher magnification, AQP4 was detected selectively at the basolateral membrane of the cells. (b, inset) Double immunolabeling using AQP4 antibody (green signal) and a monoclonal antibody for H^+/K^+ -ATPase (red signal) confirmed the selective expression of AQP4 in parietal cells. (c) In transfected cells (clone 10C1), AQP4 was located on the basolateral membrane. (d) No labeling with AQP4 antibodies was observed in wild-type HGT-1 cells. Bars: (a) 20 μm ; (b) 10 μm ; (c and d) 8 μm .



AQP4 have been detected only in parietal cells located at the base of the gastric pit in human, mouse, and rat stomach (Frigeri et al., 1995; Misaka et al., 1996; Wang et al., 2000). It has been suggested that this particular spatial location of AQP4 would be consistent with a specialization of parietal cell functions during their lifespan (Karam, 1993; Kressin, 1996). The parietal cells located at the base of the gastric pit would secrete less acid and more water. Although the evidence for the expression of an AQP itself does not prove functionally significant, the presence of AQP4 supports a role of AQPs in gastric fluid transport. In cultured rabbit parietal cells, Sonnentag et al. (2000) observed volume changes during stimulation of acid secretion followed by regulatory volume increase, which is predominantly mediated by Na^+/H^+ and Cl^-/HCO_3^- exchangers. This finding suggests that water intake into parietal cells is necessary or at least concurrent with stimulation of acid secretion. On the other hand, a recent finding from AQP4 knockout mice (Wang et al., 2000) showed that AQP4 deletion was not associated with changes in the rates of basal or stimulated acid or fluid secretion. However, these data do not rule out the possibility that other compensatory mechanisms might be responsible for the absence of obvious defects in overall gastric acid production in AQP4 knockout mice.

The goal of this study was to determine whether stimulation of acid secretion might directly or indirectly regulate the AQP4 water channel in gastric parietal cells. To this end, we exploited HGT-1, the cell line derived from a human gastric adenocarcinoma. The HGT-1 cell line is similar to

parietal cells in that it possesses functional histamine H_2 receptor (Laboisse et al., 1982), the principal receptor involved in the stimulation of acid secretion. In a recent study (Carmosino et al., 2000), we extended the characterization of HGT-1 cells as a culture model of gastric parietal cells, demonstrating that HGT-1 cells express a functional histamine-regulated H^+/K^+ -ATPase and the principal transporters involved in the regulation of acid secretion such as the Na^+/H^+ and Cl^-/HCO_3^- exchangers. HGT-1 cells were stably transfected with the coding sequence of rat AQP4. Freeze-fracture EM revealed the presence of orthogonal arrays of particles (OAPs),* the morphological feature of AQP4 (Yang et al., 1996), in the basolateral plasma membrane of transfected cells. The OAPs visible in AQP4-transfected cells were morphologically undistinguishable from those observed in other tissues (Rash et al., 1974; Orci et al., 1981; Hatton and Ellisman, 1982; Hirsch et al., 1988; Zampighi et al., 1989).

Here, we show that a deep modification of AQP4 assembly in OAPs at the basolateral membrane occurs after 20 min of histamine stimulation, which is associated with a parallel decrease of water transport. Of note, in HGT-1 cells it has been shown that the histamine effect declines after a 20–30-min exposure (Prost et al., 1984) due to an attenuation

*Abbreviations used in this paper: AQP, aquaporin; b-AQP, biotinylated AQP; HGT, human gastric tumor cell line; IBMX, 3-isobutyl-1-methylxanthine; IMP, intramembrane particle; OAPs, orthogonal arrays of particles; PAO, phenylarsine oxide; TIR, total internal reflection.

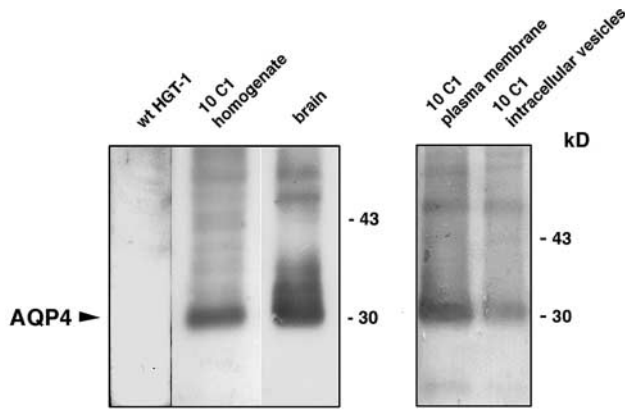


Figure 2. Immunoblot of cell homogenate and membrane fractions from rat brain or AQP4-transfected cells. Each lane was loaded with 60 μ g proteins. A single band of 30 kD without glycosylation was detected in AQP4-transfected cell homogenate and in native rat brain membranes, the positive control. A prominent expression of AQP4 in the fraction enriched in plasma membrane (17,000 g pellet) was observed compared with the expression in the fraction enriched in intracellular vesicles (200,000 g pellet).

of the receptor responsiveness, whereas the maximal hormonal effect occurs at early time points (5–10 min).

Beside the observation of OAPs absence or the marked decrease in a variety of hereditary and acquired diseases (Hutton and Ellisman, 1984; Suzuki et al., 1984; Wakayama et al., 1989; Neuhaus et al., 1990), this is the first evidence for a short term rearrangement of OAPs in an established AQP4-expressing cell line.

Results

Expression of AQP4 in rat stomach and in transfected cells

Immunofluorescence localization of AQP4 in rat stomach was carried out using a polyclonal antibody directed against a peptide corresponding to the COOH terminus of the rat AQP4. A strong signal was found along the glandular base region of the fundic gland but not in the epithelial region facing the gastric lumen or in the neck region (Fig. 1 a). The

cells positive for the AQP4 protein were parietal cells, as assessed by double labeling with H^+/K^+ -ATPase (Fig. 1 b, inset). This pattern of staining was similar to that found in human (Misaka et al., 1996) and in mouse (Wang et al., 2000) stomach, consistent with the theory that parietal cells in the base of the gastric pits have a major role in water transport compared with the more superficial parietal cells.

HGT-1 cells stably transfected with the cDNA corresponding to the encoding region of rat AQP4 were analyzed for AQP4 expression, localization, and function. A selected clone, referred to as 10C1 clone, was used for all the experiments. Clonal cells expressing AQP4 had identical growth characteristics and morphology to untransfected cells. The localization of AQP4 in 10C1 cells was examined by immunofluorescence. Expressed AQP4 protein was confined at the basolateral membrane (Fig. 1 c) thus displaying a similar distribution to that in native parietal cells in the rat stomach (Fig. 1, a and b). Untransfected wild-type HGT-1 cells were neither stained with the immune (Fig. 1 d) nor with the pre-immune serum (unpublished data).

Immunoblot analysis demonstrated that the anti-AQP4 antibody stained a single nonglycosylated band of 30 kD in 10C1 cell homogenate similar to native rat brain membranes used as a positive control (Fig. 2). No bands were detected when wild-type HGT-1 cell homogenate was probed with immune serum (Fig. 2). Subcellular fractionation of 10C1 cells was carried out to confirm the plasma membrane expression of AQP4. Immunoblot analysis showed prominent expression of AQP4 in the fraction enriched in plasma membranes (17,000 g pellet) compared with the expression in the fraction enriched in intracellular vesicles (200,000 g pellet) (Fig. 2), consistent with a predominant plasma membrane expression of AQP4.

To examine the osmotic permeability properties of transfected cells, functional analysis were carried out on cells grown on glass coverslips. Fig. 3 A shows the time course of cell swelling in response to changes in perfusate osmolality measured by a phase-contrast technique. Cells were subjected to a 200-mOsm inwardly direct gradient of NaCl. The gradient caused cell swelling, which produced a decrease in transmitted light intensity. The experiments were performed at 20°C to reduce the contribution of diffusional water permeability. The rate of cell swelling was

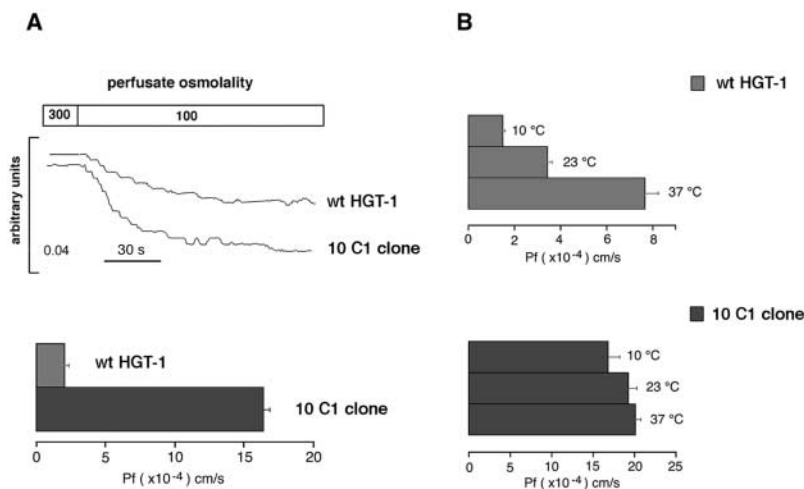


Figure 3. Osmotic water permeability properties of wild-type HGT-1 cells and 10C1 cells measured by phase-contrast technique. (A) Time course of a cell swelling in response to the change in perfusate osmolality (top). Mean value \pm SE of osmotic permeability coefficient P_f of HGT-1 and 10C1 cells (bottom). (B) Temperature dependence of HGT-1 and 10C1 osmotic water permeability coefficient.

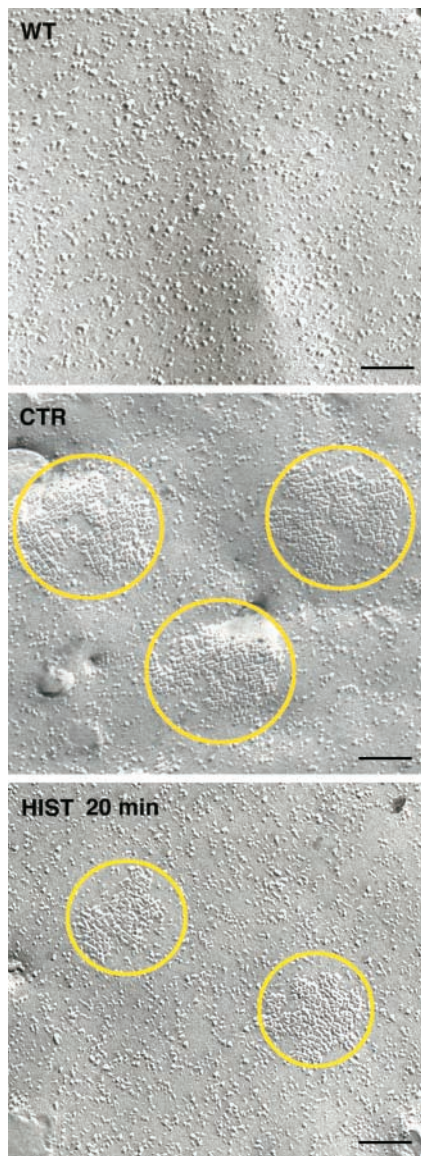


Figure 4. Freeze-fracture electron micrographs of the plasma membrane of wild-type (WT), control (CTR), and histamine-stimulated 10C1 cells (HIST 20 min). Typical OAPs were visible in the plasma membrane of control 10C1 cells (CTR). After 20 min of histamine stimulation, the density and number of OAPs decreased compared with control (HIST 20 min). Bars, 100 nm.

significantly different in wild-type and transfected 10C1 clonal cells (Fig. 3 A). Calculated osmotic water permeability coefficient P_f in 10C1 cells was eightfold that obtained from wild-type HGT-1 cells (from $2.02 \pm 0.3 \times 10^{-4}$ to $16.37 \pm 0.5 \times 10^{-4}$ cm/s; Fig. 3 A). These results are consistent with the expression of functional AQP4 water channels in 10C1 cells. The effect of temperature on the P_f in wild-type and transfected cells was determined at 10, 23, and 37°C. No significant temperature dependence was observed in 10C1 cells, suggesting a channel-mediated water transport (Fig. 3 B).

Histamine stimulation induces rearrangements of OAPs in AQP4-transfected cells

Freeze-fracture EM of AQP4-transfected cells revealed OAPs on the cytoplasmic leaflet (P-face) (Fig. 4, CTR) typical of AQP4 (Yang et al., 1996). OAPs were never observed on wild-type HGT1 cells (Fig. 4, WT).

The center-to-center spacing of the P-face grooves was ~ 8 nm, as also reported in other heterologous systems expressing AQP4 water channels (Yang et al., 1996).

We next analyzed the effect of forskolin (10 min, 100 μ M), and histamine (10 or 20 min, 100 μ M) stimulation on OAPs organization in AQP4-transfected cells. Quantitative morphometry was carried out on ≥ 10 separate cells from each experimental condition. Total OAPs surface area and total OAPs number obtained from the examination of the total cell surface area (CTR, 260 μ m²; FK, 10 min, 252 μ m²; HIST 10 min, 259 μ m²; HIST 20 min, 249 μ m²) are reported in the top part of the Table I (raw data).

The calculated OAPs density (surface area occupied by OAPs expressed as the percentage of the total surface area examined) was $2.5 \pm 0.3\%$ under basal condition (Table I; processed data). The OAPs density ($P = 0.004$) decreased significantly by $\sim 50\%$ to $1.2 \pm 0.3\%$ after 20 min histamine stimulation due to a significant decrease in OAPs number per μ m² together with a decrease in average OAPs size (Table I; Fig. 4, HIST 20 min). Compared with the control, no significant modification either in the density or in the number of OAPs was observed after 10 min of histamine treatment (Table I; processed data).

Forskolin treatment did not significantly modify the OAPs density (Table I; processed data, $2.1 \pm 0.4\%$), although in several cells a tendency to have an increase in the average size of OAPs was observed in this experimental condition (Table I; processed data).

Table I. Quantitative morphometry of AQP4-transfected cells, clone 10C1

Raw data	CTR	FK 10 min	HIST 10 min	HIST 20 min
	<i>n</i> = 10	<i>n</i> = 10	<i>n</i> = 14	<i>n</i> = 10
Surface area examined (μ m ²)	260	252	259	249
Total OAPs surface area (μ m ²)	6.70	5.38	5.99	2.80
Total number of OAPs	202	131	194	103
Processed data	CTR	FK 10 min	HIST 10 min	HIST 20 min
OAPs density (%)	2.5 ± 0.3	2.1 ± 0.4	2.9 ± 0.9	1.2 ± 0.3^a
Number of OAPs per μ m ²	0.75 ± 0.08	0.53 ± 0.09	0.90 ± 0.22	0.43 ± 0.1^b
OAPs size (μ m ²)	0.034 ± 0.003	0.040 ± 0.004	0.032 ± 0.004	0.028 ± 0.003

^a $P = 0.004$ compared to control (Student's *t* test for unpaired data).

^b $P = 0.02$ compared to control (Student's *t* test for unpaired data).

Table II. Comparison of P-face IMP density

Cell type	Density of IMP ($\text{IMPs}/\mu\text{m}^2$)	Surface area (μm^2)
wt HGT-1	2591 \pm 161 (9)	1.37
10C1 ctr	2367 \pm 138 (10)	1.52
10C1 hist	2269 \pm 95 (10)	1.52

IMPs were measured on cell plasma membranes. Values are mean \pm SE, with the number of cell in parentheses.

These results suggest that a regulation of AQP4 assembly in the basolateral membrane occurs after 20 min of exposure to histamine. The dramatic reduction (50%) in OAPs density observed after 20 min of histamine stimulation might result from AQP4 endocytosis in an intracellular compartment. An alternative explanation is that AQP4 disassemble into discrete intramembrane particles (IMPs). In an attempt to answer this question, the number of IMPs was calculated in 10 different cells (total surface examined was $1.52 \mu\text{m}^2$) after 20 min of histamine stimulation and compared with both wild-type ($n = 9$, total surface examined was $1.37 \mu\text{m}^2$) and control-transfected cells ($n = 10$, total surface examined was $1.52 \mu\text{m}^2$). Table II summarizes the obtained results. No difference in the number of IMPs was observed in either experimental condition. Although these results rather favor the possibility that AQP4 is internalized after 20 min of histamine stimulation, it has to be pointed out that the high density of IMPs found in wild-type cells might mask the appearance of a new population of IMPs deriving from OAPs disassembly, and this method might not have the sufficient resolution to give an unequivocal explanation of the real mechanism involved. Therefore, cell surface biotinylation was carried out to semiquantitate the expression levels of AQP4 in the basolateral membrane in control and histamine-stimulated cells. Biotinylated proteins were visualized by fluorescence staining using avidin-FITC under basal conditions (Fig. 5 A, ctr), after stimulation with histamine $100 \mu\text{M}$ for 20 min (Fig. 5 A, hist 20 min), or after stimulation with histamine in cells preincubated with $80 \mu\text{M}$ phenylarsine oxide (PAO), an inhibitor of several cell surface receptor endocytosis including histamine H_2 receptors (Hertel et al., 1985; Feldman et al., 1986; Garland et al., 1994; Smit et al., 1995). A clear staining lining the basolateral membrane was observed in control cells without any apparent intracellular labeling, indicating that sulfo-NHS-biotin did not enter the cells. In contrast, a considerable decrease of the cell surface staining was observed in cells exposed to histamine for 20 min, indicating that cell surface protein endocytosis occurs after this period time. In addition, some intracellular punctate staining was observed beneath the cell surface in this experimental condition likely matching protein endocytosis (Fig. 5 A, hist 20 min). No apparent intracellular labeling was observed in cells stimulated with histamine after a preincubation with the inhibitor of receptor endocytosis PAO. These results suggest that surface biotinylated proteins are internalized at long time histamine exposure (20 min).

Fig. 5 B shows a representative experiment of cell surface biotinylation. Biotinylated proteins were immunoblotted and probed with AQP4 antibody. Band intensities of biotinylated AQP4 (b-AQP4) were semiquantitated by densitometric analysis and reported as the percentage of the inten-

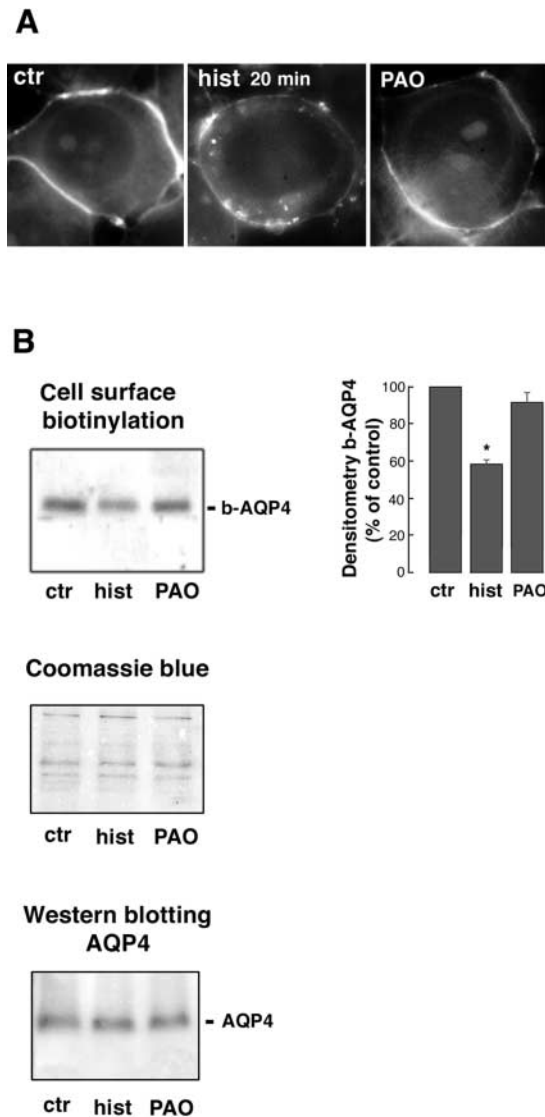


Figure 5. **Cell surface biotinylation.** (A) Cells grown on coverslips were incubated with sulfo-NHS-biotin as described in Materials and methods. Then, cells were either left under basal conditions (ctr), stimulated with histamine $100 \mu\text{M}$ for 20 min (hist 20 min), or stimulated with histamine after a 10-min preincubation with $80 \mu\text{M}$ PAO, an inhibitor of the H_2 receptor endocytosis (Smit et al., 1995). For visualization of biotinylated proteins, cells were fixed in methanol and stained with avidin-FITC (1:200). A clear staining lining the basolateral membrane was observed in control cells without any apparent intracellular labeling. In contrast, most of the cell surface staining disappeared in cells exposed to histamine for 20 min. Some intracellular punctate staining was observed beneath the cell surface. No apparent intracellular labeling was observed in cells stimulated with histamine after a preincubation with the inhibitor of receptor endocytosis PAO.

(B) Representative experiment of cell surface biotinylation. Cells grown on Petri dishes were incubated with sulfo-NHS-biotin as described in Materials and methods. Biotinylated proteins were immunoblotted and probed with AQP4 antibody. Band intensities of b-AQP4 were semiquantitated by densitometric analysis and reported as the percentage of the intensity of the band detected in the control sample (right). After 20 min of histamine stimulation, the amount of b-AQP4 decreased by $41\% \pm 2.02$ ($P = 0.004$, $n = 3$, Student's t test for paired data). No significant reduction of b-AQP4 was observed in the PAO-treated sample. Coomassie blue staining of biotinylated proteins confirmed the presence of comparable amounts of proteins in all samples. Western blot analysis of equal amounts of the solubilized starting material (cell lysates after biotinylation) from each condition confirmed the presence of comparable amount of AQP4 in all samples.

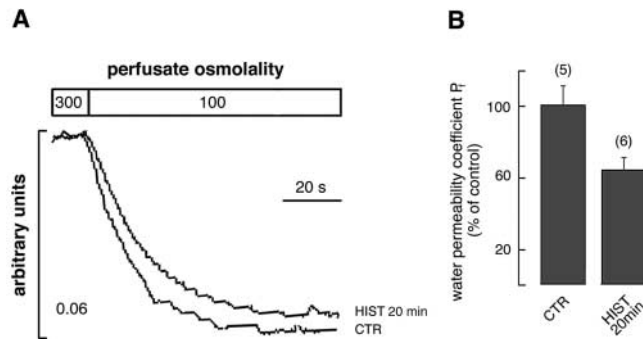


Figure 6. Effect of 20 min of histamine stimulation on the osmotic water permeability coefficient P_f . (A) Representative TIR fluorescence time course of control (CTR) and histamine-stimulated (HIST 20 min) transfected cells in response to a 200 mOsm inwardly directed NaCl gradient at 20°C. (B) Means \pm SE of P_f values calculated as percentage where 100% represents the P_f of control cells. Histamine stimulation (100 μ M, 37°C, 20 min), determined a significant (35.6% \pm 6.5, $P = 0.02$) decrease of the P_f compared with control cells (number of determinations in parentheses).

sity of the band detected in the control sample (Fig. 5 B, right). After 20 min of histamine stimulation, the amount of b-AQP4 decreased by 41% \pm 2.02 (means \pm SE; $P = 0.004$, Student's t test for paired data). No significant reduction of b-AQP4 was observed in PAO-treated samples. No bands were detected in cells treated identically without the addition of biotin during the biotinylation step (unpublished data). Coomassie blue staining of biotinylated proteins confirmed the presence of comparable amounts of proteins in all samples. Western blot analysis of equal amounts of the solubilized starting material (cell lysates after biotinylation) from each condition confirmed the presence of comparable amount of AQP4 in all samples.

Together, these findings indicate that AQP4 internalization is the actual mechanism, explaining the OAPs reduction after 20 min of histamine stimulation. If less AQP4 is present on the basolateral membrane after 20 min of histamine exposure, we would expect a parallel reduction in the osmotic water permeability coefficient (P_f). Functional analysis of water permeability was conducted on control and histamine-stimulated AQP4-transfected cells. Fig. 6 A reports a representative time course of cell swelling in response to changes in perfusate osmolality measured by total internal reflection (TIR) microfluorimetry. Relative to control (CTR), the osmotic water permeability coefficient P_f was significant inhibited by 35.6% \pm 6.54 (means \pm SE; $P = 0.02$, Student's t test for unpaired data) after 20 min of treatment (Fig. 6 B, HIST 20 min). No significant modification of the P_f was observed in AQP4-transfected cells treated with either histamine or forskolin for 10 min (unpublished data).

Discussion

We have demonstrated recently that HGT-1 cells share several physiological features with gastric parietal cells (Carmosino et al., 2000). HGT-1 cell monolayers were able to secrete H^+ when stimulated with histamine, and intracellular pH (pHi) measurements demonstrated the expression

of a functional omeprazole-sensitive H^+/K^+ -ATPase (Carmosino et al., 2000).

Together, those observations validate HGT-1 cells as an interesting cell culture model for studying the regulatory mechanisms involved in acid secretion. To this end, HGT-1 cells were stably transfected with AQP4, and OAPs, the morphological feature of the AQP4 water channel were quantitatively assessed after stimulation of acid secretion with histamine.

The major finding of this work was the observation of a marked (50%) decrease in the density of OAPs in histamine-stimulated transfected cells. The effect was observed after 20 min of histamine stimulation, a time point at which exposure of cells to the agonist results in attenuation (desensitization) of the subsequent cellular response (Prost et al., 1984). Consistent with this observation, functional studies demonstrated nearly a 35% decrease in the osmotic water permeability coefficient after 20 min of histamine stimulation (Fig. 6). These findings support the hypothesis that activation of the H_2 receptor in the basolateral membrane leads eventually to a rearrangement of the AQP4 assembly in the basolateral membrane of gastric parietal cells.

A possible explanation for this effect is that AQP4 might switch from an assembled (OAPs) to a disassembled (discrete IMPs) state, which might reflect a different functional state of the water channel. Recent finding by van Hoek et al. (2000) would support this possibility. In mouse kidney, the authors found a strong immunofluorescence AQP4 labeling in epithelial cells of the S3 segment, whereas freeze-fracture analysis revealed the presence of a small number of OAPs (van Hoek et al., 2000). As van Hoek et al. (2000) suggested, these data raise the possibility that AQP4 has less tendency to form OAPs in the proximal tubule and might be present also as discrete IMPs, either monomers or tetramers.

Attempts to estimate the number of single particles representing AQP4 showed no obvious increase in the number of IMPs after 20 min of histamine stimulation (Table II), although this method might not have the sufficient resolution to give an unequivocal answer. Therefore, we exploited an alternative strategy of semiquantitation of the amount of AQP4 on the cell surface by cell surface biotinylation (either assembled in OAPs or existing as a "single particle") and allowing to distinguish between an aggregation/disaggregation model or AQP4 endocytosis. Indeed, biotinylation studies confirmed that 20 min of histamine exposure induces a nearly 40% reduction of cell surface b-AQP4, and this effect is accompanied with internalization of surface-biotinylated proteins.

We might speculate that AQP4 is internalized together or concomitantly with the H_2 receptor after 20 min of histamine stimulation. Our finding, demonstrating that after a 20-min stimulation with histamine in cells preincubated with PAO, an inhibitor of several cell surface receptor endocytosis, including histamine H_2 receptors (Hertel et al., 1985; Feldman et al., 1986; Garland et al., 1994; Smit et al., 1995), would support this hypothesis. Several observations by other authors would also favor this possibility. First, in HGT-1 cells it has been demonstrated that short term treatment of cells with histamine produced a progressive decline in the subsequent efficacy of histamine on H_2 receptor activity, and after only 20 min the response was reduced to 50%

of the control response (Prost et al., 1984). This effect was not related to cAMP levels nor to adenylate cyclase activity, suggesting that the decrease in histamine H₂ receptor activity may be produced by uncoupling of the receptor to the adenylate cyclase or receptor internalization into a compartment inaccessible to agonists acting at the plasma membrane. Several guanine nucleotide-binding protein-coupled receptors have been reported to be internalized (Prost et al., 1984; Arima et al., 1993; Fukushima et al., 1993, 1996; Smit et al., 1994). The likely mechanism for the decrease in histamine H₂ receptor activity is the receptor internalization. In fact, in COS7 cells transfected with canine H₂ receptor (Fukushima et al., 1997) the amount of cell surface H₂ receptor detected with antibody binding decreased by ~30% after a 30-min incubation with histamine. Second, in HEK-293 cells transfected with the H₂ receptor a 1-h treatment with histamine resulted in an almost complete disappearance of H₂ receptor immunoreactivity, whereas a 1-h incubation with forskolin did not lead to important changes of membrane-localized H₂ immunoreactivity (Smit et al., 1995). This indicates that histamine causes H₂ receptor internalization via a cAMP-independent pathway. Of note, forskolin stimulation of AQP4-transfected cells did not cause any significant modification both in the density and in the number of OAPs compared with the control condition. If AQP4 is internalized in a cAMP-independent manner, forskolin exposure of cells is not expected to induce any modification of the OAPs at the basolateral membrane.

Third, by freeze-fracture EM Bordi et al. (1986) described OAPs reduction (nearly 50%) in native gastric parietal cells of rat stomach after pentagastrin and metiamide treatment. Since these findings were obtained in native parietal cells, this supports our hypothesis that the arrays can be modulated by parietal cell function. Moreover, the apparent discrepancy found by authors regarding the reduction in OAPs both in response to exposure of cells to treatments that stimulate (pentagastrin, which in turn activates histamine release) or inhibit (metiamide, an H₂ receptor antagonist) gastric secretion might be explained again by OAPs internalization concurrent to H₂ receptor internalization. In fact, disappearance of histamine receptor activity was also observed with the H₂ receptor antagonist SKF 93479 (Prost et al., 1984), thus suggesting that occupancy of the H₂ receptor is the key event triggering the inactivation.

Based on these considerations, we may speculate that tight control of signaling via H₂ receptor activation/internalization associated with regulation of OAPs appearance (possibly recycling) on the membrane would in turn regulate gastric secretion.

A working model hypothesizing a transcellular water transport would imply that subsequent to activation of acid secretion water could enter through AQP4 at the basolateral membrane by simple osmosis. At early time points (10 min), histamine or forskolin treatments did not induce significant modifications to the density or number of OAPs, nor to the P_f , and thus the constitutive water permeability of the basolateral membrane of gastric parietal cells would not represent a limiting barrier for water transport. Longer histamine exposure (20 min) eventually leads to a downregulation of water transport through AQP4 internalization concomitantly to the H₂ receptor.

A transcellular pathway for water secretion implies that water must leave the apical membrane for the formation of gastric juice. So far, no water channel has been detected in the apical membrane (Koyama et al., 1999). However, one possible pathway for water to exit is through apical cotransport protein (Zeuthen, 1994; Zeuthen and Stein, 1994) in an otherwise impermeable membrane (Priver et al., 1993). Alternatively, other unknown AQPs may mediate water exit from the apical membrane.

To conclude, this study demonstrates that in AQP4-transfected gastric cells, endocytosis of the water channel AQP4, matched by 50% OAPs reduction, occurs after 20 min of histamine exposure. This effect is paralleled by a reduction of the osmotic water permeability coefficient P_f and coincides with the 50% attenuation of the hormonal response observed in those cells (Prost et al., 1984), likely due to histamine receptor internalization (Fukushima et al., 1997). Although the exact relationship between the secretory activity and biochemical events examined here is complex, we propose that the parallel downregulation of histamine response and cell surface AQP4 expression evidenced in AQP4-transfected cells could be involved in the physiological control of gastric cell function.

Materials and methods

Materials

Polyclonal antibodies specific for rat AQP4 were raised against the synthetic peptide corresponding to the 15 COOH-terminal amino acids of rat AQP4 (amino acids 278–301, EKGKDSSGEVLSSV) as described previously (Valenti et al., 1996). The monoclonal antibody 2AG11 against the β -subunit of H⁺/K⁺-ATPase was a gift from Dr. Forte (Department of Molecular and Cell Biology, University of California, Berkeley, CA). Anti-rabbit IgG FITC conjugate and anti-mouse IgG Cy3 conjugate were obtained from Sigma-Aldrich. Chemicals were obtained from the following sources: histamine, 3-isobutyl-1-methylxanthine (IBMX), and forskolin were purchased from Sigma-Aldrich, lipofectin and geneticin were purchased from Life Technologies, and sulfo-NHS-biotin and streptavidin-agarose beads were purchased from Pierce Chemical Co.

Cell culture

HGT-1 cells derive from a poorly differentiated human gastric adenocarcinoma (Laboisse et al., 1982) and display the characteristic of gastric parietal cells (Laboisse et al., 1982; Sandle et al., 1993). Cells were cultured at 37°C under a humidified atmosphere of 5% CO₂-95% air in DME (high glucose) supplemented with 20 mM sodium bicarbonate, 20 mM Hepes, and 10% FCS without antibiotics.

Plasmid construction and transfection

The cDNA coding for rat lung AQP4 cDNA was amplified by PCR and ligated into expression vector pcDNA3 containing the cytomegalovirus promoter and the gene for resistance to geneticin.

The primers (sense, 5'-GCTGATCATGGTGGCTTTCAAAGGC-3'; anti-sense, 5'-GCTCTAGATACAGAAGATAATACCTC-3') were engineered with BclI (5') and XbaI (3') restriction sites. The BclI and XbaI fragment was ligated into the vector at BamHI and XbaI restriction sites and propagated in *Escherichia coli*. Transfection was performed by use of lipofectin. HGT-1 (wild-type) cells were grown at 37°C under a humidified atmosphere of 5% CO₂-95% air in DME supplemented with 20 mM sodium bicarbonate, 20 mM Hepes, and 10% FCS without antibiotics. Cells were plated into 45-mm dishes for 15 h before transfection. Cells were washed with serum-free medium and then incubated for 12 h at 37°C with 2 ml of serum-free medium containing 20 μ g of lipofectin and 5 μ g of recombinant plasmid. Cells were washed and then grown for 48 h in DME supplemented with 10% FCS. Cells were trypsinized and plated on 140 mm-diameter dishes. A selection of cells containing transfected DNA was obtained with a medium containing geneticin (500 μ g/ml) for 10–15 d. Resistant clones were isolated and transferred to separate culture dishes for expansion and analysis.

Subcellular fractionation

Cells grown on a 25-cm² flask to confluency were scraped with a policeman, pelleted, and resuspended in 30 μ l of lysis buffer (50 mM Tris, pH 8, 110 mM NaCl, 0.5% Triton X-100, 0.5% Nonidet P-40, 2 mM PMSF, 2 μ g/ml leupeptin and pepstatin), vortexed vigorously, and incubated at 4°C for 60 min. The cell lysate was clarified with a brief centrifugation and resuspended in Laemmli buffer. For the preparation of the low speed pellet enriched in plasma membranes (LSP) and the high speed pellet enriched in intracellular vesicles (HPS), the cells were washed in PBS and homogenized with a glass/Teflon homogenizer in ice-cold buffer containing 250 mM sucrose and 10 mM Tris, pH 7.5. Cell suspension was centrifuged at 700 *g* for 10 min at 4°C. The supernatant was centrifuged at 17,000 *g* for 45 min at 4°C. The LSP was recovered in PBS, and the supernatant was spun at 200,000 *g* in a Beckman Coulter Rotor 50 2Ti for 60 min at 4°C. The final pellet (HSP) was recovered in PBS. Cell membranes were stored at -20°C until used for immunoblotting studies. For brain crude membrane preparation, rat brains were removed, cut into small slices, and homogenized in ice-cold buffer containing 300 mM mannitol and 12 mM Hepes-Tris, pH 7.4. All subsequent steps were performed at 4°C. The suspension was centrifuged at 2,500 *g* for 15 min to discard nuclei and unbroken cells. The supernatant was spun down at 47,000 *g* for 45 min, and the pellet was resuspended in homogenizing buffer.

Immunoblot analysis

Membranes or cell homogenates were solubilized in Laemmli buffer, heated to 60°C for 10 min, and subjected to 13% SDS-PAGE. Gels were transferred to Immobilon-P membrane (Millipore), blocked in blotting buffer (150 mM NaCl, 20 mM Tris-HCl, pH 7.4, and 1% Triton X-100) containing 5% nonfat dry milk for 1 h. The membranes were incubated with the AQP4 polyclonal antibody (1:400 dilution) for 2 h at room temperature in blotting buffer and washed in several changes of the same blotting buffer. The membranes were incubated with goat rabbit IgG (1:5,000 dilution; Sigma-Aldrich) and revealed with anti-mouse alkaline-phosphatase using the substrates 0.56 mM 5-bromo-4-chloro-3-indolyl phosphate and 0.48 mM nitro blue tetrazolium in 10 mM Tris-HCl, pH 9.5.

Cell surface biotinylation

To semiquantify the expression levels of AQP4 in the basolateral membrane, cell surface biotinylation experiments were performed. AQP4-transfected cells were grown on 4-cm Petri dishes, washed with PBS-Ca²⁺/Mg²⁺, and either left untreated or stimulated with histamine 100 μ M plus IBMX 100 μ M for 20 min at 37°C, or stimulated with histamine after a 10-min preincubation with 80 μ M PAO, an inhibitor of several cell surface receptor endocytosis including histamine H₂ receptors (Hertel et al., 1985; Feldman et al., 1986; Garland et al., 1994; Smit et al., 1995). Cells were then washed with ice-cold PBS-Ca²⁺/Mg²⁺ and incubated with 1 mg/ml sulfo-NHS-biotin in PBS Ca²⁺/Mg²⁺ for 30 min at 4°C. Free sulfo-NHS-biotin was blocked by washing cells twice at 4°C with 0.1 M glycine in PBS-Ca²⁺/Mg²⁺ and then with ice-cold PBS-Ca²⁺/Mg²⁺. Cells were lysed in lysis buffer (110 mM NaCl, 50 mM Tris, 0.5% Triton X-100, 0.5% Igepal, pH 8, 1 mM phenylmethylsulfonyl fluoride, 1 μ g/ml pepstatin, and 1 μ g/ml leupeptin), and extracts were clarified by centrifugation (13,000 *g* for 10 min). An equal volume of Streptavidin-agarose beads was added to the lysates (400 μ g of proteins), and the mixture was incubated with gentle mixing at 4°C overnight. Streptavidin-bound complexes were pelleted and washed three times with 500 μ l lysis buffer. Biotinylated proteins were eluted in Laemmli buffer by boiling for 10 min, resolved by SDS-PAGE, electroblotted onto Immobilon-P, and immunoblotted with the AQP4 antibody (1:400 dilution). Band intensities were quantitated by densitometric analysis using National Institutes of Health Image software.

Light microscopy immunocytochemistry

Cells grown on glass coverslips were fixed in ice-cold methanol for 5 min. After blocking in 0.1% gelatin in PBS for 5 min, cells were incubated at room temperature for 2 h with the primary antibody (IS AQP4, dilution 1:200). After washing three times for 5 min with 0.1% gelatin, cells were incubated for 1 h with FITC-conjugated secondary antibodies, and then were sequentially washed twice for 1 min in 2.7% NaCl (high salt PBS) and twice in regular PBS. Coverslips were mounted in 50% glycerol in 0.2 M Tris-HCl, pH 8.0, containing 2.5% *n*-propyl gallate as an anti-quenching agent. For the immunofluorescence study on the rat stomach, small samples of rat stomach were fixed in a fixative containing 2% paraformaldehyde, 10 mM sodium periodate, and 75 mM lysine (PLP) at 4°C overnight. The samples were then infiltrated in 30% sucrose for 3 h and mounted in OCT medium (Miles), frozen in liquid nitrogen, and sectioned at 4- μ m thickness on a Reichert Frigocut cryostat. Sections were placed on

Superfrost/plus microscope slides (Fisher Scientific) and subjected to immunofluorescence as described above. For double immunolabeling of AQP4 and H⁺/K⁺-ATPase in rat stomach, sections were incubated sequentially with the monoclonal antibody against the β -subunit of H⁺/K⁺-ATPase (1:200) and the polyclonal antibody against AQP4 (1:200). Anti-mouse Cy3-conjugated IgG (1:200) and anti-rabbit FITC-conjugated IgG (1:100) were used, respectively, as secondary antibodies. For fluorescence visualization of biotinylated proteins, cells grown on coverslips were incubated with sulfo-NHS-biotin (1 mg/ml in PBS-Ca²⁺/Mg²⁺ for 30 min at 4°C). Free sulfo-NHS-biotin was blocked by washing cells twice at 4°C with 0.1 M glycine in PBS-Ca²⁺/Mg²⁺ and then with ice-cold PBS-Ca²⁺/Mg²⁺. Then, cells were either left under basal conditions, stimulated with histamine 100 μ M plus IBMX 100 μ M for 20 min at 37°C, and in parallel stimulated with histamine after a 10-min preincubation with 80 μ M PAO, an inhibitor of H₂ receptor endocytosis (Smit et al., 1995). Cells were fixed in methanol and stained with avidin-FITC (1:200 dilution).

The slides were examined with a Leica photomicroscope equipped for epifluorescence, and digital images were obtained by a cooled CCD camera interfaced to the microscope (Princeton Instruments).

Water transport assay

Water permeability in adherent cells was measured by a phase-contrast technique based on volume-dependent changes in optical path length of light passing through a cell monolayer (Farinas et al., 1997). Cells were grown to confluence on 18-mm glass coverslips and then mounted in a specific chamber. Cells were illuminated and visualized using a 20 \times objective. Transmitted light was collected and focused onto a photomultiplier. The osmotic water permeability was determined from the time course of the interference signal in response to osmotic gradients. Alternatively, cell volume changes on adherent cells were measured by TIR fluorimetry as described previously (Valenti et al., 1996). Experimental conditions included control cells (CTR) and 100 μ M histamine plus 100 μ M IBMX for 20 min at 37°C (HIST 20 min). The osmotic water permeability coefficient (P_f) was calculated from the exponential time constant τ by the relation $P_f = [\tau (A/V)_0 V_w \Phi_0]^{-1}$, where $(A/V)_0$ is the initial cell surface-to-volume ratio, V_w is the partial molar volume of water (18 cm³/mol), and Φ_0 is the initial perfusate osmolality. Cell surface-to-volume ratio was calculated from serial confocal images of calcein-loaded cells by the MRC-1024 Bio-Rad Laboratories confocal microscope equipped with a krypton-argon-mixed gas laser. A specific software (Imaris 2.7; Bitplane) was used for acquisition and processing of confocal images.

Freeze-fracture EM

Cells grown on 25-cm² flasks were left under basal conditions or stimulated with either 100 μ M histamine (10 or 20 min) or 100 μ M forskolin (15 min) in the presence of 100 μ M IBMX. Then, cell monolayers were fixed for 20 min with 2% glutaraldehyde, rinsed, and stored in PBS-Na₂S₂O₃. Monolayers were scraped and cryoprotected in 30% glycerol. Cells suspension were deposited on freeze-fracture supports and frozen by immersion in Freon 22 cooled with liquid nitrogen. Specimens were fractured at -130°C in a Balzers freeze-fracture device and were shadowed by depositing platinum at an angle of 45° followed by carbon at 90%. Replicas were cleaned in bleach and distilled water. Replicas were collected on EM grids and examined and photographed using a Philips EM400 electron microscope. Experimental conditions included: control cells (CTR), 100 μ M histamine plus 100 μ M IBMX for 10 min at 37°C (HIST 10 min), 100 μ M histamine plus 100 μ M IBMX for 20 min at 37°C (HIST 20 min), and 100 μ M forskolin plus 100 μ M IBMX for 10 min at 37°C (FK).

We thank Dr. A. Frigeri for his expert contribution in the cell transfection. We thank Dr. C.L. Labois (Inserm, 94-04, Faculte de Medecine, Nantes, France) for providing the HGT-1 cells, clone 6. We thank our colleague Anthony Green for providing linguistic advice.

This work was supported by a grant from European Union, Training and Mobility of Researchers network (proposal ERB 4061 PL 97-0406), and from the Italian Ministero della Ricerca Scientifica e Tecnologica (Università degli Studi, Bari, Italy).

Submitted: 5 March 2001

Accepted: 2 August 2001

References

Arima, N., Y. Kinoshita, A. Nakamura, Y. Yamashita, and T. Chiba. 1993. Homologous desensitization of histamine H₂ receptors in the human gastric

- carcinoma cell line MKN-45. *Am. J. Physiol.* 265:G987–G992.
- Bordi, C., M. Amherdt, and A. Perrelet. 1986. Orthogonal arrays of particles in the gastric parietal cell of the rat: differences between superficial and basal cells in the gland and after pentagastrin or metiamide treatment. *Anat. Rec.* 215: 28–34.
- Carmosino, M., G. Procino, V. Casavola, M. Svelto, and G. Valenti. 2000. The cultured human gastric cells HGT-1 express the principal transporters involved in acid secretion. *Pflugers. Arch.* 440:871–880.
- Farinas, J., M. Kneen, M. Moore, and A.S. Verkman. 1997. Plasma membrane water permeability of cultured cells and epithelia measured by light microscopy with spatial filtering. *J. Gen. Physiol.* 110:283–296.
- Feldman, R.D., W. McArdle, and C. Lai. 1986. Phenylarsine oxide inhibits agonist-induced changes in photolabeling but not agonist-induced desensitization of the beta-adrenergic receptor. *Mol. Pharmacol.* 30:459–462.
- Frigeri, A., M.A. Gropper, F. Umenishi, M. Kawashima, D. Brown, and A.S. Verkman. 1995. Localization of MIWC and GLIP water channel homologs in neuromuscular, epithelial, and glandular tissues. *J. Cell Sci.* 108:2993–3002.
- Fukushima, Y., Y. Oka, H. Katagiri, T. Saitoh, T. Asano, H. Ishihara, N. Matsuhashi, T. Kodama, Y. Yazaki, and K. Sugano. 1993. Desensitization of canine histamine H₂ receptor expressed in Chinese hamster ovary cells. *Biochem. Biophys. Res. Commun.* 190:1149–1155.
- Fukushima, Y., T. Asano, H. Katagiri, M. Aihara, T. Saitoh, M. Anai, M. Funaki, T. Ogihara, K. Inukai, N. Matsuhashi, et al. 1996. Interaction between the two signal transduction systems of the histamine H₂ receptor: desensitizing and sensitizing effects of histamine stimulation on histamine-dependent cAMP production in Chinese hamster ovary cells. *Biochem. J.* 320:27–32.
- Fukushima, Y., T. Asano, K. Takata, M. Funaki, T. Ogihara, M. Anai, K. Tsukuda, T. Saitoh, H. Katagiri, M. Aihara, et al. 1997. Role of the C terminus in histamine H₂ receptor signaling, desensitization, and agonist-induced internalization. *J. Biol. Chem.* 272:19464–19470.
- Garland, A.M., E.F. Grady, D.G. Payan, S.R. Vigna, and N.M. Bunnett. 1994. Agonist-induced internalization of the substance P (NK1) receptor expressed in epithelial cells. *Biochem. J.* 301:177–186.
- Hatton, J.D., and M.H. Ellisman. 1982. The distribution of orthogonal arrays in the freeze-fractured rat median eminence. *J. Neurocytol.* 11:335–349.
- Hatton, J.D., and M.H. Ellisman. 1984. Orthogonal arrays are redistributed in the membranes of astroglia from alumina-induced epileptic foci. *Epilepsia.* 25: 145–151.
- Hertel, C., S.J. Coulter, and J.P. Perkins. 1985. A comparison of catecholamine-induced internalization of beta-adrenergic receptors and receptor-mediated endocytosis of epidermal growth factor in human astrocytoma cell. Inhibition by phenylarsine oxide. *J. Biol. Chem.* 260:12547–12553.
- Hirsch, M., D. Gache, and W. Noske. 1988. Orthogonal arrays of particles in non-pigmented cells of rat ciliary epithelium: relation to distribution of filipin- and digitonin-induced alterations of the basolateral membrane. *Cell Tissue Res.* 252:165–173.
- Karam, S.M. 1993. Dynamics of epithelial cells in the corpus of the mouse stomach. IV. Bidirectional migration of parietal cells ending in their gradual degeneration and loss. *Anat. Rec.* 236:314–332.
- Koyama, Y., T. Yamamoto, T. Tani, K. Nihei, D. Kondo, H. Funaki, E. Yaoita, K. Kawasaki, N. Sato, K. Hatakeyama, et al. 1999. Expression and localization of aquaporins in rat gastrointestinal tract. *Am. J. Physiol.* 276:C621–C627.
- Kressin, M. 1996. Heterogeneity and migration-related zonation of K(+)-ATPase activities in the oxyntic cell lineage of adult cattle. *Cell Tissue Res.* 284:231–238.
- Laboisie, C.L., C. Augeron, M.H. Couturier-Turpin, C. Gespach, A.M. Cheret, and F. Potet. 1982. Characterization of a newly established human gastric cancer cell line HGT-1 bearing histamine H₂-receptors. *Cancer Res.* 42: 1541–1548.
- Ma, T., and A.S. Verkman. 1999. Aquaporin water channels in gastrointestinal physiology. *J. Physiol.* 517:317–326.
- Misaka, T., K. Abe, K. Iwabuchi, Y. Kusakabe, M. Ichinose, K. Miki, Y. Emori, and S. Arai. 1996. A water channel closely related to rat brain aquaporin 4 is expressed in acid- and pepsinogen-secretory cells of human stomach. *FEBS Lett.* 381:208–212.
- Neuhaus, J., E.M. Schmid, and H. Wolburg. 1990. Stability of orthogonal arrays of particles in murine skeletal muscle and astrocytes after circulatory arrest, and human gliomas. *Neurosci. Lett.* 109:163–168.
- Orci, L., F. Humbert, D. Brown, and A. Perrelet. 1981. Membrane ultrastructure in urinary tubules. *Int. Rev. Cytol.* 73:183–242.
- Priver, N.A., E.C. Rabon, and M.L. Zeidel. 1993. Apical membrane of the gastric parietal cell: water, proton, and nonelectrolyte permeabilities. *Biochemistry.* 32:2459–2468.
- Prost, A., S. Emami, and C. Gespach. 1984. Desensitization by histamine of H₂ receptor-mediated adenylate cyclase activation in the human gastric cancer cell line HGT-1. *FEBS Lett.* 177:227–230.
- Rash, J.E., L.A. Staehelin, and M.H. Ellisman. 1974. Rectangular arrays of particles on freeze-cleaved plasma membranes are not gap junctions. *Exp. Cell Res.* 86:187–190.
- Sandle, G.I., G. Fraser, K. Fogg, and G. Warhurst. 1993. Properties of a potassium channel in cultured human gastric cells (HGT-1) possessing specific omeprazole binding sites. *Gut.* 34:1331–1338.
- Smit, M.J., R. Leurs, S.R. Shukrula, A. Bast, and H. Timmerman. 1994. Rapid desensitization of the histamine H₂ receptor on the human monocytic cell line U937. *Eur. J. Pharmacol.* 288:17–25.
- Smit, M.J., H. Timmerman, A.E. Alewijnse, M. Punin, I. van den Nieuwenhof, J. Blauw, J. van Minnen, and R. Leurs. 1995. Visualization of agonist-induced internalization of histamine H₂ receptors. *Biochem. Biophys. Res. Commun.* 214:1138–1145.
- Sonnentag, T., W.K. Siegel, O. Bachmann, H. Rossmann, A. Mack, H.J. Wagner, M. Gregor, and U. Seidler. 2000. Agonist-induced cytoplasmic volume changes in cultured rabbit parietal cells. *Am. J. Physiol. Gastrointest. Liver Physiol.* 279:G40–G48.
- Suzuki, M., Y. Iwasaki, T. Yamamoto, H. Konno, T. Yoshimoto, and J. Suzuki. 1984. Disintegration of orthogonal arrays in perivascular astrocytic processes as an early event in acute global ischemia. *Brain Res.* 300:141–145.
- Valenti, G., A. Frigeri, P.M. Ronco, C. D'Errorre, and M. Svelto. 1996. Expression and functional analysis of water channels in a stably AQP2-transfected human collecting duct cell line. *J. Biol. Chem.* 271:24365–24370.
- van Hoek, A.N., T. Ma, B. Yang, A.S. Verkman, and D. Brown. 2000. Aquaporin-4 is expressed in basolateral membranes of proximal tubule S3 segments in mouse kidney. *Am. J. Physiol. Renal Physiol.* 278:F310–F316.
- Wakayama, Y., T. Jimi, N. Misugi, T. Kumagai, S. Miyake, S. Shibuya, and T. Miike. 1989. Dystrophin immunostaining and freeze-fracture studies of muscles of patients with early stage amyotrophic lateral sclerosis and Duchenne muscular dystrophy. *J. Neurol. Sci.* 91:191–205.
- Wang, K.S., A.R. Komar, T. Ma, F. Filiz, J. McLeroy, K. Hoda, A.S. Verkman, and J.A. Bastidas. 2000. Gastric acid secretion in aquaporin-4 knockout mice. *Am. J. Physiol. Gastrointest. Liver Physiol.* 279:G448–G453.
- Yang, B., D. Brown, and A.S. Verkman. 1996. The mercurial insensitive water channel (AQP-4) forms orthogonal arrays in stably transfected Chinese hamster ovary cells. *J. Biol. Chem.* 271:4577–4580.
- Zampighi, G.A., J.E. Hall, G.R. Ehrling, and S.A. Simon. 1989. The structural organization and protein composition of lens fiber junctions. *J. Cell Biol.* 108: 2255–2275.
- Zeuthen, T. 1994. Cotransport of K⁺, Cl⁻ and H₂O by membrane proteins from choroid plexus epithelium of *Necturus maculosus*. *J. Physiol.* 478:203–219.
- Zeuthen, T., and W.D. Stein. 1994. Cotransport of salt and water in membrane proteins: membrane proteins as osmotic engines. *J. Membr. Biol.* 137:179–195.